ISSN: 2472-3703 DOI: 10.6911/WSRJ.202605_12(5).0001

Synaptic Plasticity of Memristors Based on ZnO Thin Films Fabricated by PLD

Yanxia Liang, Jianbiao Chen*, Shuangju Jia, Lizhi Zhang, Mingrui Liu, Xuhui Tian, Tao Ye, Hongyu Li

Key Laboratory of Atomic & Molecular Physics and Functional Materials of Gansu Province, College of Physics and Electronic Engineering, Northwest Normal University, Lanzhou, 730070, China

* Corresponding Author: E-mail address: jbchen@nwnu.edu.cn

Abstract

Cu/ZnO/Cu memristive devices with planar-structure were successfully fabricated using pulsed laser deposition (PLD) technology by regulating substrate temperature. At a substrate temperature of 500 °C, ZnO thin film of the device exhibits smooth and uniform surface morphology demonstrated by systematic characterization. Such memristive devices show excellent dynamic resistive switching behavior under electrical pulse stimulation, with their resistance states capable of being precisely modulated by the polarity, amplitude, and duration of electrical pulses. Leveraging this tunable resistive switching property, the devices successfully emulate various biological synaptic behaviors including excitatory postsynaptic current and paired-pulse facilitation, demonstrating promising potential for applications in neuromorphic computing.

Keywords

Memristor; Synaptic Plasticity; Resistance Switching; ZnO; PLD.

1. INTRODUCTION

Memristors are a research hotspot in brain-inspired neuromorphic networks due to their synapse-like structure, non-volatile properties, and ability to mimic synaptic functions while enabling in-memory computing. Memristors typically adopt a metal/insulator (semiconductor)/metal (MIM) "sandwich" structure, which mainly includes two configurations: vertically stacked and planar architectures. The planar two-terminal memristor features a simpler structure with advantages of compact size and high integration density. Under electrical stimulation, the insulating (semiconducting) layer between metal electrodes generally exhibits two distinct resistive states: high-resistance state (HRS) and low-resistance state (LRS),[1] whose transitions can be modulated by applying bias voltage across the terminals. These devices are considered the most promising next-generation non-volatile memory because of their short response time, low energy consumption,[2] simple structure, and high integration density. However, as a hardware technology with just over a decade of physical development, memristors still face challenges before achieving large-scale real-world applications. To optimize memristor performance, critical factors involve not only the selection of appropriate resistive switching materials and electrode materials, but also the assembly and integration of device structures.

Zinc oxide (ZnO), as a widely used semiconductor material, possesses a direct bandgap of 3.37 eV and an exciton binding energy of 60 meV at room temperature.[3-5] Additionally, ZnO exhibits high electron mobility and excellent thermal stability, making it extensively applicable

ISSN: 2472-3703 DOI: 10.6911/WSRJ.202605_12(5).0001

in optoelectronic fields. Its inherent properties give it unique potential as a resistive switching material for memristors.

In recent years, various research teams have developed diverse ZnO-based memristors and employed multiple approaches to optimize and regulate device performance. An Ag(Al)/ZnO/WO_x/FTO memristor was fabricated to enhance device performance using magnetron sputtering by optimizing sputtering process parameters, including annealing and oxygen supply.[6-9] Through nitrogen doping and adjustment of ZnO film thickness, nitrogen-doped ZnO memristors were prepared via magnetron sputtering to modulate memristive behavior. Furthermore, Prof. Wang Shaoxi's team introduced a TiO_2 interlayer to achieve unipolar-enhanced bilayer and unipolar-weakened monolayer memristors. They also developed a dual-transistor-dual-memristor (2T2R) unit capable of exhibiting long-term potentiation (LTP) and long-term depression (LTD) characteristics under unipolar voltage pulse stimulation.[10]

These memristive devices have potential applications in various fields. Wang Li et al. modeled a lab-fabricated ZnO memristor and proposed a novel double-layer reservoir computing architecture based on ZnO memristors for digital identification tasks.[11-13] The Ag(Al)/ZnO/WO_x/FTO memristor designed and fabricated by Xizi Qin et al. is a memristor-based emotion monitoring system, this system can identify and record negative emotions by detecting crying sounds and heartbeat signals. Pan Jie et al. employed radio-frequency (RF) magnetron sputtering to fabricate WO_x-ZnO memristors. These devices exhibit biologically inspired synaptic properties suitable for neuromorphic computing and artificial intelligence (AI) hardware. These advancements demonstrate that research on ZnO memristors has reached a mature stage, with synaptic emulation and neural training emerging as a cutting-edge yet challenging focus.[14-18] Nevertheless, ZnO-based memristors still exhibit several notable limitations that hinder their practical applications. Firstly, fabrication process inconsistencies remain a critical issue, as thin films prepared by different methods (e.g., sol-gel and magnetron sputtering) demonstrate significant performance variations with poor batch-to-batch reproducibility. Solution-based approaches, particularly wet chemical methods like sol-gel, are highly sensitive to precursor purity and annealing conditions, often resulting in films with excessive porosity and insufficient density. Moreover, the high equipment costs associated with precision techniques such as atomic layer deposition (ALD) pose challenges for large-scale manufacturing. The fabricated devices also suffer from unstable resistive switching behavior due to the random migration of oxygen vacancies (Vo), which leads to uncontrolled conductive filament formation and necessitates further improvement in cycling endurance ($>10^6$ cycles).[19-21] Environmental sensitivity is another concern, as the susceptibility of ZnO to moisture and oxygen degradation requires additional encapsulation layers, thereby increasing process complexity. In terms of neuromorphic applications, these devices face challenges in synaptic emulation, including nonlinear conductance modulation (manifested in non-ideal LTP/LTD curves) that compromises artificial neural networks (ANNs) training accuracy, limited dynamic range (typically $G_{max}/G_{min}<50$) falling short of ideal synaptic device requirements (>100), and insufficient temporal matching in spike-timing-dependent plasticity (STDP) response speed (μs-ms scale) compared to biological synapses. These limitations collectively underscore the need for further material optimization and device engineering to realize the full potential of ZnO memristors in neuromorphic computing systems.[22-24]

The pulsed laser deposition (PLD) technique demonstrates remarkable advantages in fabricating ZnO-based memristors owing to its unique physical deposition mechanism. Specifically, PLD enables the growth of ZnO thin films with high crystallinity (preferred c-axis orientation) and low defect density through laser-ablated high-energy plasma deposition, which significantly enhances resistive switching stability. This technique allows precise stoichiometric control by adjusting laser energy and oxygen partial pressure to regulate oxygen

ISSN: 2472-3703 DOI: 10.6911/WSRJ.202605_12(5).0001

vacancy concentration, thereby optimizing the reliability of conductive filament formation/rupture.[25-28] Furthermore, the clean deposition process facilitates the formation of atomically smooth ZnO/electrode (e.g., Pt and ITO) interfaces with minimal contamination, effectively reducing interfacial barrier effects on device performance. Notably, the superior film uniformity achieved by PLD promotes more linear conductance modulation and improved symmetry in LTP/LTD curves, while the high-energy deposition may create nanocrystalline/amorphous hybrid structures that potentially enhance the spatiotemporal dynamics matching of STDP.[29-31]

Building upon these advantages, this work provides a Cu/ZnO/Cu planar memristor with excellent crystallinity and low defect density through optimized substrate temperature using PLD. The developed device not only simplifies the conventional MIM vertical architecture but also maintains compact dimensions and high integration density. Its stable resistive switching characteristics and dynamic synaptic emulation capabilities provide new perspectives for neuromorphic hardware development. This work achieves controllable fabrication of high-performance electronic synapses through process-structure-property co-optimization, providing a neuromorphic computing and brain-inspired AI hardware platform capable of simulating complex neurodynamic.

2. EXPERIMENTAL PREPARATION

A 1 cm×1 cm silicon wafer containing a 280 nm oxide layer was cut as a substrate. The substrate was cleaned with isopropyl alcohol, acetone, and ethanol for 10 min in sequence, and then placed in the vacuum chamber of the PLD system after the surface of the substrate was air-dried. The ZnO target was placed 5 cm away from the substrate, and all the valves of the vacuum chamber were closed. The experimental procedure began with the activation of the mechanical pump and bypass valve, followed by two minutes waiting period before opening the vacuum gauge. Upon observing the vacuum gauge reading drop below 20 Pa, the bypass valve was closed while the electromagnetic isolation valve was opened. After stabilization of the vacuum gauge readings, the gate valve was subsequently opened. The molecular pump was then started and maintained until reaching a stable operating frequency of 600 Hz. When the chamber pressure achieves 5×10^{-4} Pa, the laser system was activated with predetermined parameters: an excitation voltage of 27 kV, frequency of 10 Hz, and pulse count of 3000. Concurrently, the substrate heating system was engaged to maintain the desired deposition temperature, with five predetermined temperature settings (100, 200, 300, 400, and 500 °C, respectively) employed for experimental comparison.

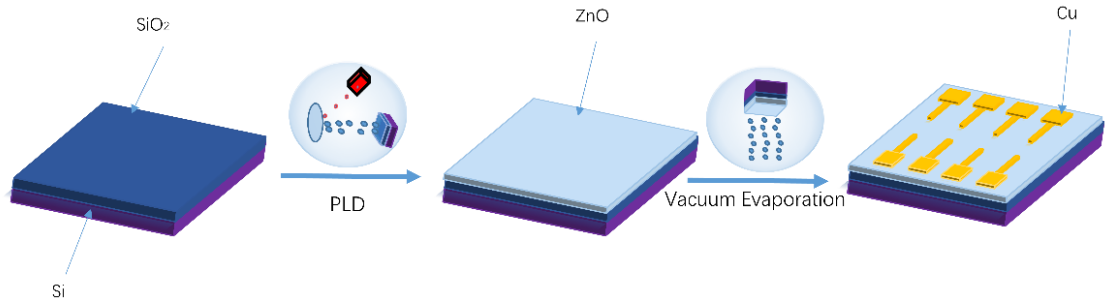

Figure 1. Schematic diagram of the process of preparing Cu/ZnO/Cu memristor assisted by PLD method

Upon reaching the target temperature, simultaneous rotation of both substrate and target was initiated prior to commencing thin-film deposition via pulsed laser ablation. Following

ISSN: 2472-3703 DOI: 10.6911/WSRJ.202605_12(5).0001

deposition completion, the laser system was deactivated and the vacuum system was systematically shut down. The substrate undergoes natural cooling before extraction of the ZnO-coated silicon wafer. The final fabrication step involved deposition of metallic copper electrodes at both device terminals under a working pressure of 2.1×10^{-3} Pa, with a controlled 50 μm interelectrode spacing to complete the planar memristor structure.

3. CHARACTERISATION OF CU/ZNO/CU MEMRISTRS

3.1. Structural analysis of ZnO films

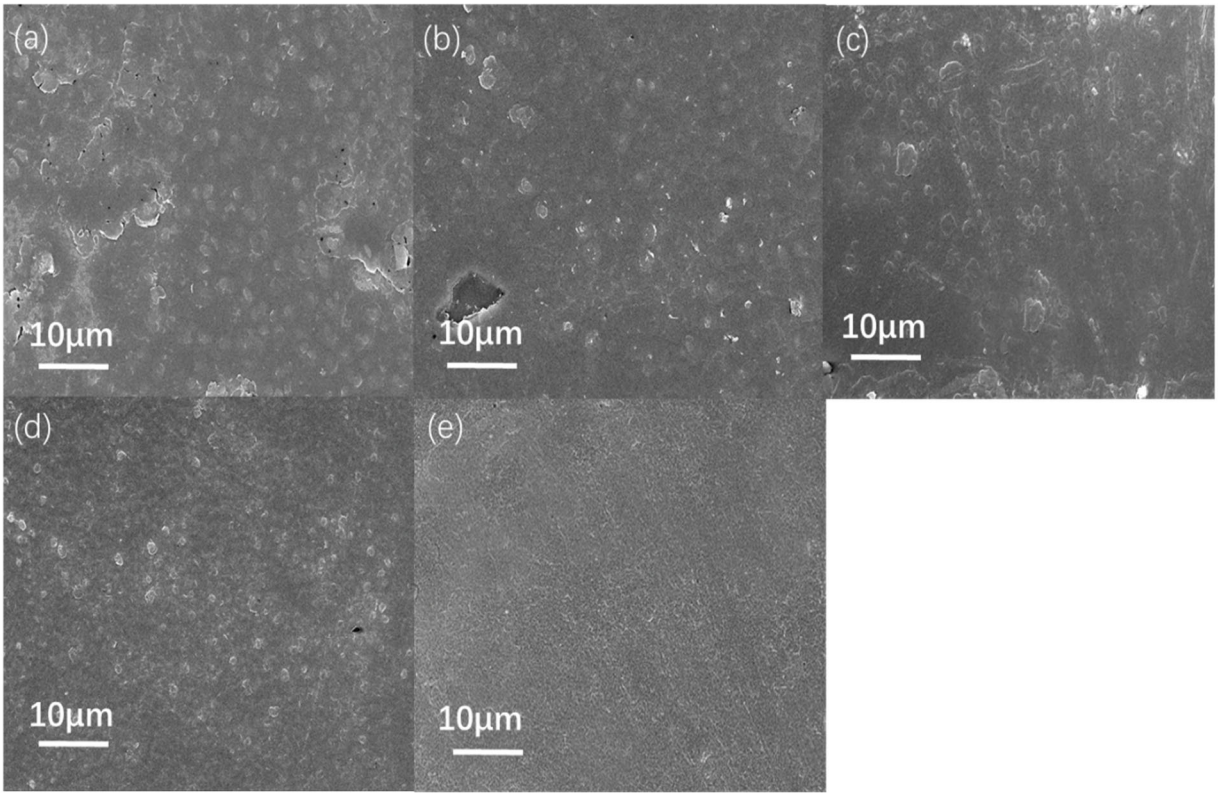

Figure 2. The surface SEM images of ZnO thin films at deposition temperatures of (a) 100, (b) 200 , (c) 300, (d) 400, and (e) 500 °C, respectively

Figure 2 presents the surface SEM images of ZnO thin films deposited at different temperatures. As the deposition temperature increases from 100 to 500 ℃, the film surface becomes progressively smoother and more uniform, as evidenced by the surface SEM image obtained at 500 ℃ (Figure 3 (a)). Cross-sectional analysis reveals tha the ZnO film thickness is approximately 137 nm (Figure 3 (b)). As shown in Figure 3 (c), high-resolution TEM reveals lattice fringes with an interplanar spacing of 0.2395 nm, which corresponds to the (101) plane of ZnO through calculation. Furthermore, the electron diffraction pattern in Figure 3 (d) clearly demonstrates the presence of (110), (102), (101) and (002) crystal planes of ZnO, confirming the formation of nanocrystalline ZnO.

ISSN: 2472-3703 DOI: 10.6911/WSRJ.202605_12(5).0001

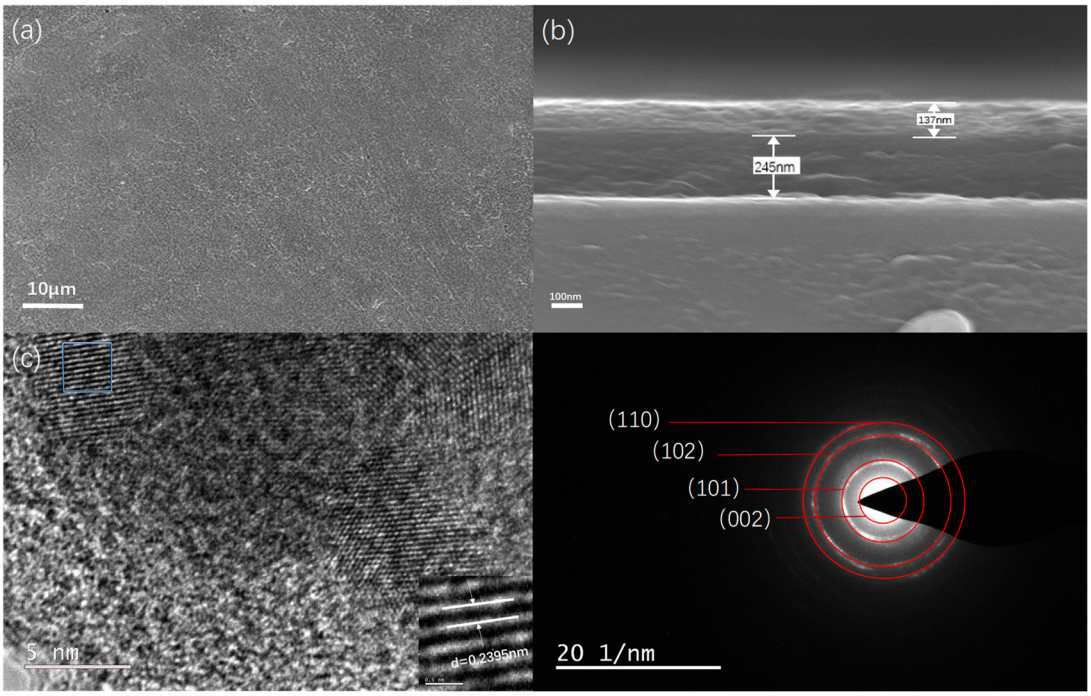

Figure 3 (a) Surface and (b) cross-sectional SEM image, (c) high-resolution TEM image, and (d) selected area electron diffraction pattern of ZnO thin films deposited at 500 °C

The microstrain (ε) in zinc oxide thin films can be quantitatively characterized by the following relationship:

$$\varepsilon = (1/4)\beta_{2\theta}\cos\theta \quad (1)$$

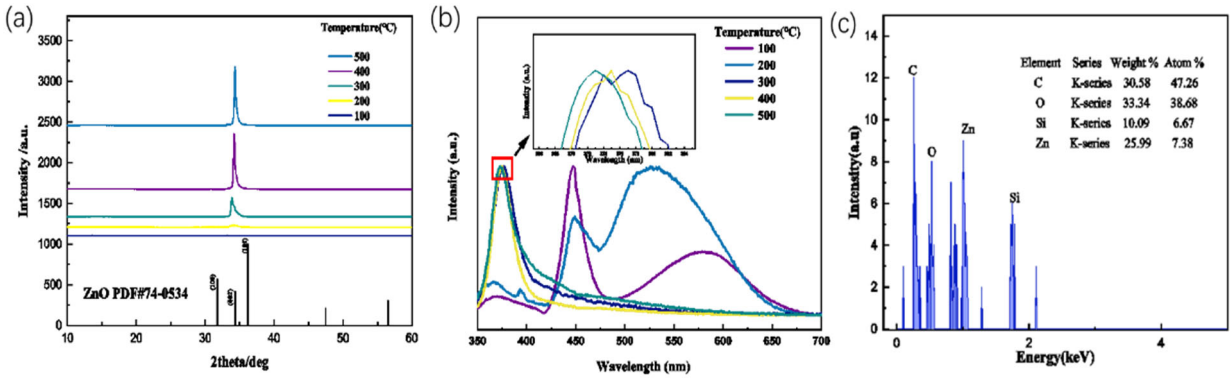

Figure 4 (a) XRD patterns, (b) PL spectra, and (c) selected area EDS analysis of ZnO thin films prepared by PLD at different deposition temperatures

Where $\beta_2\theta$ represents the full width at half maximum (FWHM) of the (002) diffraction peak in the XRD pattern. The specific FWHM fitting values at different temperatures are shown in Table 1. As the temperature increases from 100 °C to 500 °C, the FWHM values gradually decrease, corresponding to a reduction in microstrain. This notable lattice relaxation effect demonstrates that high-temperature deposition facilitates the elimination of lattice distortions in the films, thereby yielding ZnO films with more complete crystallization and lower defect density.

ISSN: 2472-3703 DOI: 10.6911/WSRJ.202605_12(5).0001

As shown in Figure 4 (a), ZnO thin films prepared at different substrate temperatures all exhibit significant (002) preferential orientation characteristics. With increasing deposition temperature, the (002) diffraction peaks systematically shift toward higher angles, with peak positions eventually approaching the reference value (2θ=34.42°) from the standard PDF card (JCPDS No.74-0534). This phenomenon indicates that optimizing substrate temperature can effectively regulate the lattice parameters of ZnO films, bringing them closer to the theoretical values of ideal wurtzite structure. These conclusions are consistent with the aforementioned SEM characterization results.

Table 1. Half peak width of XRD pattern (002) peak of ZnO thin films at different deposition temperatures

Temperature (°C)	w
100	2.0596 ± 0.37717
200	1.22745 ± 0.01104
300	0.44535 ± 0.00386
400	0.32288 ± 0.00159
500	0.2728 ± 0.00137

Figure 4 (b) presents the photoluminescence (PL) spectra of the ZnO thin films. All samples exhibit characteristic ZnO emission peaks in the 350-400 nm range, confirming the successful formation of zinc oxide. Notably, films deposited at lower substrate temperatures(100-200 °C) show additional defect-related emission bands in the visible region: blue (430-455 nm), green (500-550 nm), and yellow (550-600 nm) emissions, which are well-documented in references. In contrast, films grown at higher temperatures (300-500 °C) display only the intrinsic ZnO emission without these defect-related peaks. The inset highlights an interesting phenomenon: the main emission peak undergoes a systematic blue shift with increasing deposition temperature. This spectral shift indicates a corresponding increase in both the emission energy and the band gap of the ZnO films, suggesting improved crystalline quality and reduced defect concentration at higher growth temperatures.

Figure 4 (c) presents the selected-area energy-dispersive X-ray spectroscopy (EDS) analysis of the device. Combined with the aforementioned characterization results, these data conclusively demonstrate the successful preparation of high-quality ZnO thin films with uniform surface morphology and low defect density at the optimal deposition temperature of 500 °C.

3.2. Electrical characterisation of Cu/ZnO/Cu memristors

Figure 5 (a) shows the current-voltage (I-V) characteristics of the Cu/ZnO/Cu memristor. Under the same scanning voltage, only the device deposited at 500 °C exhibits relatively pronounced switching behavior.

To elucidate the resistive switching mechanism, logarithmic transformation was performed on the I-V characteristics. The mechanism fitting plot in Figure 5 (b) (positive voltage sweep) shows that the fitted slopes approach unity in both the high-resistance state (HRS) and low-resistance state (LRS), confirming the dominance of ohmic conduction. During the transition from HRS to LRS, the slope of the I-V curve increases to 1.3, exhibiting the characteristic square-law region of space-charge-limited current (SCLC) conduction, which indicates the presence of electron trapping in defect states within the dielectric layer.

Figure 5 (c) presents the results of the negative voltage sweep. Although the SCLC mechanism is still maintained, the square-law region exhibits a slightly steeper slope compared to the positive sweep. This discrepancy likely arises from the measurement sequence, since the

ISSN: 2472-3703 DOI: 10.6911/WSRJ.202605_12(5).0001

negative sweeps were performed after the positive ones, partial trap filling had already occurred, thereby modifying the conduction characteristics. The symmetrical I-V behavior under opposite polarities confirms the bipolar resistive switching nature of the device."**

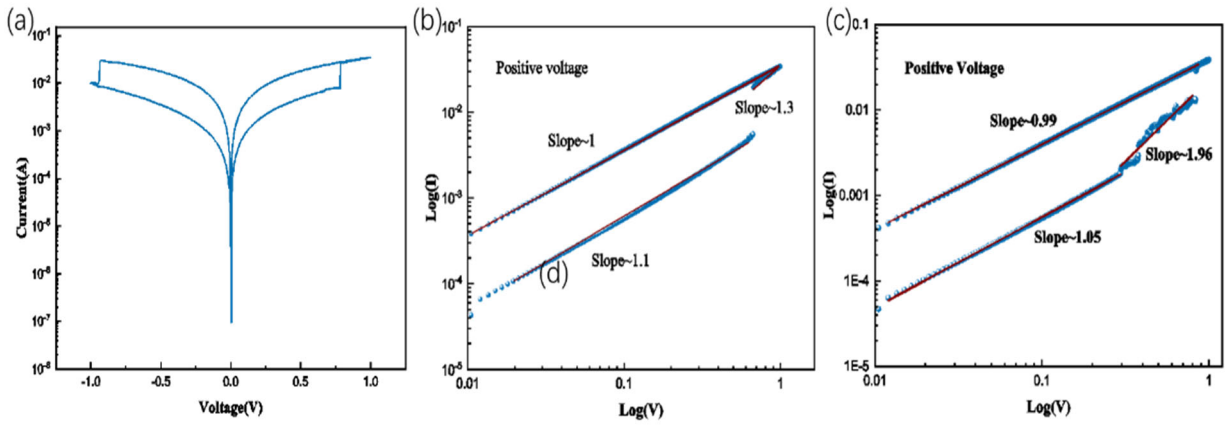

Figure 5. (a) Butterfly-shaped I-V curves of the Cu/ZnO/Cu memristor at a deposition temperature of 500 °C under a scanning voltage of 1 V, (b) Mechanism fitting curve under forward voltage sweep, and (c) reverse voltage sweep, respectively

3.3. Synaptic mimicry analysis of Cu/ZnO/Cu memristors

Cu/ZnO/Cu devices with two-terminals exhibit remarkable structural similarity to biological synapses in the human brain. Their continuously tunable resistance enables them to function as electronic synapses, accurately mimicking the signal transmission mechanism of biological synapses through modulation of interneuronal connection strength. When stimulated by presynaptic pulses (1 V, 10 ms), the device generates excitatory postsynaptic current (EPSC) with a peak amplitude of 0.075 mA, which gradually decay to a resting current of -0.125 mA (Figure 6 (a)). This electrophysiological behavior precisely replicates the process of action potential propagation along axons and synaptic transmission in biological neural systems.

Short-term synaptic enhancement was achieved using paired presynaptic pulse stimulation (inter-pulse interval: 0.01-0.02 ms). As shown in Figure 6 (a), the peak amplitude of the second EPSC reaches 1.42 times that of the first, attributable to residual current superposition before complete decay. Figure 6 (b) demonstrates the variation of the paired-pulse facilitation (PPF) index with inter-pulse interval Δt. The PPF effect gradually weakens as Δt increases and disappears completely when Δt exceeds the characteristic decay time, reflecting the device stimulus forgetting characteristics. These results highlight the potential of Cu/ZnO/Cu memristors for emulating biological short-term plasticity. Further optimization through pulse parameter engineering may advance neuromorphic computing applications based on this novel material platform.

STDP, a fundamental synaptic characteristic, is defined as the relative change in synaptic weight (ΔW) induced by presynaptic and postsynaptic pulses with varying time intervals (Δt). The temporal difference Δt = tpre - tpost, and the synaptic weight change is calculated as:

$$\Delta W = (G_{post} - G_{pre})/G_{pre} \times 100\% \quad (2)$$

ISSN: 2472-3703 DOI: 10.6911/WSRJ.202605_12(5).0001

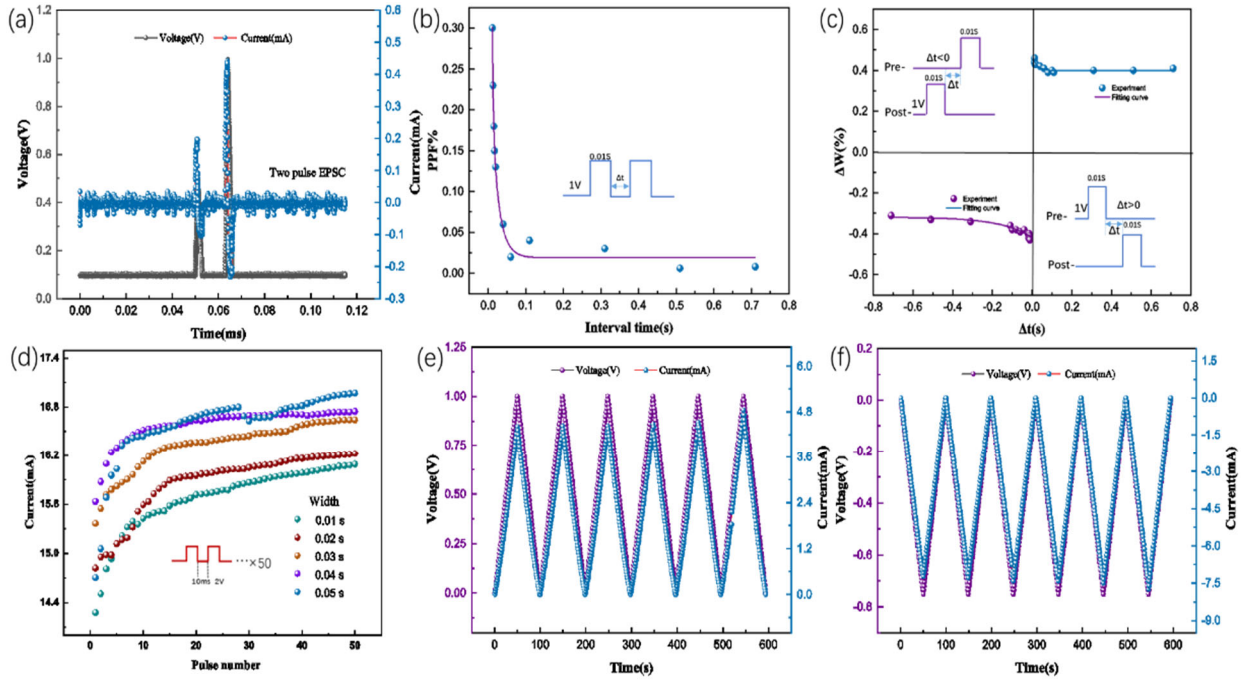

Figure 6. Artificial synaptic behaviors based on Cu/ZnO/Cu memristor: (a) EPSC response induced by paired-pulse stimulation; (b) PPF as a function of time interval between adjacent pulses, with inset showing the applied pulse scheme (amplitude: 1 V, width: 0.01 s); (c) Conductance (weight) variation of the Cu/ZnO/Cu device versus Δt, where Δt represents the time interval between presynaptic and postsynaptic stimulations. Inset: the presynaptic and postsynaptic pulse scheme (amplitude: 1 V, width: 0.01 s); (d) Schematic diagram of stimulation response pulses with different pulse widths applied to the memristor; Current response of the device under six periodic stimulations of (e) positive and (f) negative triangular pulses stimulation, respectively.

Where Gpost and Gpre represent the conductances of postsynaptic and presynaptic neurons, respectively. When presynaptic stimulation precedes postsynaptic stimulation ($\Delta t > 0$), synaptic potentiation occurs ($\Delta W > 0$); conversely, when postsynaptic stimulation precedes presynaptic stimulation ($\Delta t < 0$), synaptic depression occurs ($\Delta W < 0$).

In the Cu/ZnO/Cu memristor, one copper electrode serves as the presynaptic membrane while the other functions as the postsynaptic membrane. Synaptic stimulation was applied using pulses with 1 V amplitude and 0.01 s width. Figure 6(c) illustrates the variation of ΔW with Δt: for both $\Delta t > 0$ (potentiation) and $\Delta t < 0$ (depression) cases, synaptic weights show significant enhancement and suppression, respectively. Notably, smaller $|\Delta t|$ values yield larger $|\Delta W|$, demonstrating the device high sensitivity to precise timing differences. Specifically, for $\Delta t > 0$, synaptic weights exhibit pronounced LTP, for $\Delta t < 0$, the device demonstrates robust LTD.

Further analysis of Figure 6 (c) reveals more drastic $|\Delta W|$ variations within smaller $|\Delta t|$ ranges, highlighting the memristor high temporal resolution and its ability to dynamically adjust synaptic weights in response to precise spike timing. This rapid and accurate modulation closely mimics biological synaptic plasticity, establishing the Cu/ZnO/Cu memristor as an ideal candidate for neural dynamics emulation.

Figure 6 (d) characterizes LTP under pulse stimulation (pulse amplitude: 1 V, interval: 0.01 s) with varying pulse widths. After 50 identical pulses, all conditions demonstrate significant LTP characteristics. Notably, while increasing pulse width enhances LTP magnitude, the observed intensification of signal fluctuations under wider pulse conditions directly confirms the

ISSN: 2472-3703 DOI: 10.6911/WSRJ.202605_12(5).0001

resultant degradation in device stability. Figure 5(e) and 5(f) present the time-dependent voltage-current response profiles. By precisely controlling the scan duration and voltage polarity, a voltage-current correlation dynamics model is established. Experimental data show progressive current enhancement characteristics during both forward and reverse voltage sweeps. This reproducible conductance modulation behavior achieved through cyclic voltage scanning exhibits tunability analogous to synaptic weight variations, confirming the device's potential to emulate biological synaptic transmission functions.

4. CONCLUSION

The PLD preparation method, combined with a relatively high substrate temperature, can yield ZnO thin films featuring high crystallinity, few defects, and a smooth surface. The Cu/ZnO/Cu memristor, fabricated by PLD at 500 °C, showcases superior electrical properties but also remarkable synaptic emulation capabilities. It successfully achieves the STDP, PPF, LTP, and LTD behaviors of synapse. These features render the device an ideal platform for neuromorphic computing, biologically inspired neural networks, and brain-inspired artificial intelligence.

REFERENCES

[1] Q. P. Shen, J. Cheng, D. Guo, T. H. Yang: Analysis and Suppression of Electromagnetic Vibration Noise of Fractional-Slot Concentrated-Windings Interior PMSMs, IEEE Transactions on Transportation Electrification, Vol. 10 (2024), p.5270-5281.

[2] M. Z. Peresztegi, Z. Szakács, Z. Vereczkei, E. Dakó, S. Dakó, S. Lada, K. Lemes, M. Holczer, N. Farkas, J. Bajor: Mediterranean Diet Adherence in Celiac Patients: A Nested Cross-Sectional Study, Nutrients, Vol. 17 (2025), p.788.

[3] T. Endoh, H. Koike, S. Ikeda, T. Hanyu, H. Ohno: An Overview of Nonvolatile Emerging Memories—Spintronics for Working Memories, IEEE Journal on Emerging and Selected Topics in Circuits and Systems, Vol. 6 (2016), p.109-119.

[4] Y. Q. Wang, W. X. Wang, C. W. Zhang, H. Kan, W. J. Yue, J. B. Pang, S. Gao, Y. Li: A Digital–Analog Integrated Memristor Based on a ZnO NPs/CuO NWs Heterostructure for Neuromorphic Computing, ACS Applied Electronic Materials, Vol. 4 (2022), p.3525-3534.

[5] J. Tamil Illakkiya, S. Hemalatha, P. Usha Rajalakshmi, R. Oommen: Nanostructured zinc oxide thin films by spin coating technique, Emerging Materials Research, Vol. 5 (2016), p.57-61.

[6] F. Tian, W. P. Han, J. P. Hu, H. F. Wang, H. Li, F. J. Geng, T. Wei, D. Li: Oxygen vacancy-enriched bilayer flower-like structure of ZnO&NiO@C-ZnO nanorod arrays on carbon cloth with improved eletrochemical performance, Journal of Energy Storage, Vol. 72 (2023), p.108316.

[7] J. Y. Pan, T. Wu, W. H. Yang, Y. Li, J. Q. Zhang, H. Kan: ZnO-ITO/WO3−x heterojunction structured memristor for optoelectronic co-modulation neuromorphic computation, Science China Materials, Vol. 67 (2024), p.2838-2847.

[8] X. Z. Qin, J. D. Hu, H. Liu, X. Xu, F. Yang, B. Sun, Y. Zhao, M. Huang, Y. Zhang: Performance Regulation of a ZnO/WOx-Based Memristor and Its Application in an Emotion Circuit, The Journal of Physical Chemistry Letters, Vol. 14 (2023), p.3039-3046.

[9] Q. L. Tian, X. Y. Shan, J. Y. Bian, Y. K. Cheng, J. H. Zheng, Z. Q. Wang, X. N. Zhao, H. Y. Xu, Y. C. Liu: Metal oxide-based resistive switching memristors for neuromorphic computing, Journal of Materials Chemistry C, Vol. 13 (2025), p.12046-12065.

ISSN: 2472-3703 DOI: 10.6911/WSRJ.202605_12(5).0001

[10] Y. C. Wang, J. W. Zheng, Y. Y. Shang, D. Y. Guo, H. X. Wang, Z. Y. An, X. C. Chen, R. X. Huang, J. Y. Jiang, K. Sun, S. X. Wang: LTP–LTD transformation of unipolar pulse voltage-driven zinc oxide memristors via TiO2 thin layer incorporation, Journal of Materials Chemistry C, Vol. 12 (2024), p.1281-1288.

[11] X. M. Li, Z. J. Fang, X. Guo, R. X. Wang, Y. X. Zhao, W. H. Zhu, L. C. Wang, L. Zhang: Light-Induced Conductance Potentiation and Depression in an All-Optically Controlled Memristor, ACS Applied Materials, Vol. 16 (2024), p.27866-27874.

[12] M. Najafi, H. Haratizadeh: Investigation of intrinsic and extrinsic defects effective role on producing intense red emission in ZnO:Eu nanostructures, Materials Research Bulletin, Vol. 65 (2015), p.103-109.

[13] L. X. Wang, Y. J. Zhang, Z. C. Guo, Z. X. Wu, X. H. Chen, S. M. Du: Reservoir Computing-Based Design of ZnO Memristor-Type Digital Identification Circuits, Micromachines, Vol. 13 (2022), p.1700.

[14] M. Najafi, H. Haratizadeh: The effect of growth conditions and morphology on photoluminescence properties of Eu-doped ZnO nanostructures, Solid State Sciences, Vol. 41 (2015), p.48-51.

[15] C. S. Yoo, H-S. Lee: Interface-Type Ionic Memristor for Energy-Efficient Neuromorphic Hardware, ACS Applied Electronic Materials, Vol. 6 (2024), p.3013-3023.

[16] H. J. Zhang, B. Y. Jiang, C. T. Cheng, B. J. Huang, H. Zhang, R. Chen, J. Y. Xu, Y. L. Huang, H. D. Chen, W. H. Pei, Y. Chai, F. C. Zhou: A Self-Rectifying Synaptic Memristor Array with Ultrahigh Weight Potentiation Linearity for a Self-Organizing-Map Neural Network, Nano Letters, Vol. 23 (2023), p.3107-3115.

[17] W. Lillis, M. C. Hoffing, W. Burleson: Survey of Security Issues in Memristor-Based Machine Learning Accelerators for RF Analysis, Chips, Vol. 3 (2024), p.196-215.

[18] A. Kumar, K. Preeti, S. P. Singh, S. Lee, A. Kaushik, S. K. Sharma: ZnO-based hybrid nanocomposite for high-performance resistive switching devices: Way to smart electronic synapses, Materials Today, Vol. 69 (2023), p.262-286.

[19] S. Haukka: ALD Technology - Present and Future Challenges, ECS Transactions, Vol. 3 (2007), p.15-26.

[20] J. R. Nasr, D. S. Schulman, A. Sebastian, M. W. Horn, S. Das: Mobility Deception in Nanoscale Transistors: An Untold Contact Story, Advanced Materials, Vol. 31 (2018), p.173.

[21] A. S. Grenadyorov, A. A. Solovyev, K. V. Oskomov, V. S. Sypchenko: Thermal stability of a-C:H:SiOx thin films in hydrogen atmosphere, Thin Solid Films, Vol. 690 (2019), p.137531.

[22] H. S. Jang, G. H. Jeong, H. J. Lee, H. S. Shin, Y. Hwa, S-S. Chee, S. Y. Paek, J. M. Kim, B. Son, D. Kang, G. H. Ryu: A general and facile approach to flower-like ZnO fabrication, Materials Today Advances, Vol. 20 (2023), p.100424.

[23] T. D. Dongale, K. V. Khot, S. S. Mali, P. S. Patil, P. K. Gaikwad, R. K. Kamat, P. N. Bhosale: Development of Ag/ZnO/FTO thin film memristor using aqueous chemical route, Materials Science in Semiconductor Processing, Vol. 40 (2015), p.523-526.

[24] T. Ohno, T. Hasegawa, T. Tsuruoka, K. Terabe, J. K. Gimzewski, M. Aono: Short-term plasticity and long-term potentiation mimicked in single inorganic synapses, Nature Materials, Vol. 10 (2011), p.591-595.

[25] K. Saka, D. Gokcen: Bottom-up fabrication of n-ZnO-based memristor and p-Cu2O/n-ZnO heterojunction diode using electroless deposition, Journal of Materials Science: Materials in Electronics, Vol. 33 (2022), p.21811-21821.

[26] Y. J. Onofre, S. de Castro, M. P. F. de Godoy: Effect of traps localization in ZnO thin films by photoluminescence spectroscopy, Materials Letters, Vol. 188 (2017), p.37-40.

ISSN: 2472-3703 DOI: 10.6911/WSRJ.202605_12(5).0001

[27] A. Nath, M. Mishra, S. Chakrabarti: Impact of high substrate temperature on pulsed laser deposited ZnO pillars: A technological route to investigate the structural, optical and superhydrophilic properties, Applied Surface Science, Vol. 646 (2024), p.158907.

[28] A. A-G. Farrag, M. R. Balboul: Nano ZnO thin films synthesis by sol–gel spin coating method as a transparent layer for solar cell applications, Journal of Sol-Gel Science and Technology, Vol. 82 (2016), p.269-279.

[29] K. L. Yang, S. J. Yuan, Y. Q. Zhan, L. R. Zheng, F. Seoane: A Flexible Artificial Synapse for Neuromorphic System, Proc. 2018 IEEE International Conference on Electron Devices and Solid State Circuits (EDSSC), 2018, p.1-2.

[30] Q. Y. Zhang, B. B. Hou, J. Y. Zhang, X. S. Gu, Y. L. Huang, R. J. Pei, Y. K. Zhao: Flexible light-stimulated artificial synapse based on detached (In,Ga)N thin film for neuromorphic computing, Nanotechnology, Vol. 35 (2024), p.235202.

[31] J. B. Chen, C. Y. Yang, J. W. Xu, L. Y. Gao, T. T. Guo, S. J. Jia, P. Zhang, Y. F. Xiao, J. T. Chen, Y. Zhao, J. Wang, X. Q. Zhang, Y. Li: The plasticity of synaptic memristor based on 2D-MoS2 thin film prepared in large-scale by a PLD-assisted CVD method, Materials Today Communications, Vol. 35 (2023), p.105511.